International Journal of Electronics and Communication Engineering (IJECE)
Vol.1, Issue 1 Aug 2012 1-12

International Academy of Science, Engineering and Technology
Connecting Researchers; Nurturing Innovations

5.5 GHz NOTCHED ULTRA-WIDEBAND PRINTED MONOPOLE ANTENNA CHARACTERIZED BY ELECTROMAGNETIC BAND GAP STRUCTURES

AYMAN AYD R. SAAD[1], DEENA A. SALEM[2] & ELSAYED ESAM M. KHALED[3]

[1]Elec. Eng. Dept., Minia University, Minia, Egypt

[2]Microstrip Dept., Electronics Research Institute, Giza, Egypt

[3]Elec. Eng. Dept., Assit University, Assit, Egypt

ABSTRACT

This paper presents a promising design of a band–notched printed monopole antenna for ultra–wide band (UWB) applications. By properly incorporating either a slotted patch electromagnetic band gap (spEBG) structure or a parasitic strip electromagnetic bang gap (psEBG) structure in the antenna design a wide operating bandwidth from 3.7 to beyond 10.6 GHz for VSWR≤2 is obtained. Moreover a band–notched performance in the 5–6 GHz range is achieved. The proposed antenna is successfully designed and fabricated. The measured data of the proposed antenna show good agreement with the simulated results. Good impedance matching, high gain and high efficiency are obtained over the frequency band excluding the rejected band. The input admittance of the proposed antenna is modeled as a SPICE–compatible equivalent circuit using vector fitting technique, and the validity of the modeling method is verified.

KEYWORDS: Monopole Antenna; Ultra–Wideband (UWB); Band–Notch, EBG Structures; Circuit Modeling; Vector Fitting; SPICE Equivalent Circuit

INTRODUCTION

High data rate transmission with high efficiency and minimum distortion in the received signal are crucial requirements for ultra–wide band (UWB) wireless communication systems (3.1–10.6 GHz) [1–3]. These requirements are involved with UWB printed antennas design. In literature many of these antennas configurations have been proposed and developed [4–11]. However, these antennas need a band rejection filter to maintain the coexistence of the narrow band applications using portions of the same spectrum such as WLAN (5.15–5.35 GHz, 5.725–5.825 GHz). A simple method to achieve this band–rejection property is by loading the radiator with a slot. The slotted radiator should be designed to resonate at the central frequency of the required stop band.

Electromagnetic band gap (EBG) structures [12] are defined as artificial periodic (or non–periodic) structures that prevent/assist the propagation of electromagnetic waves in a specified band of frequency for all incident angles and all polarization states that directly depend on the dimensions and types of materials used to fabricate the EBGs. However, due to this characteristic, it has been utilized to be used in band rejection for UWB antennas [13]. Using printed antenna to obtain ultra–wide band characteristics incorporating planar electromagnetic band gap (EBG) structures improves the antenna performance such as increasing antenna efficiency, enhancing its gain, and minimizing the side and back lobe levels in the radiation patterns [14–16]. These enhancements for the antenna performance are due to the ability of such antennas to suppress the surface wave propagation in a specific frequency band [17].

In this paper, unlike usual method of slotted patch antennas, a new printed monopole antenna is proposed, that employs planar EBG structures to obtain and control the rejected frequency at the band of 5–6 GHz for UWB applications. The design process involves three phases; the first phase is to design a new shape of UWB printed monopole antenna. The second phase is to incorporate the designed antenna with either one of two different EBG structures to achieve the required frequency band–notched characteristic for the UWB applications. The third phase is to obtain the SPICE–compatible equivalent circuit models of the proposed antenna by using vector fitting technique. The results elucidate that the EBG structures exhibit well–behaved band stop characteristics required for UWB applications. Descriptions of the antenna architecture are given in Section 2. The antenna performance and characteristics are obtained and discussed in Sections 3. A SPICE–compatible equivalent circuit models of the proposed antenna is established in Section 4. Finally, the conclusion is outlined in Section 5.

ANTENNA DESIGN

The geometry of the proposed prototype antenna is illustrated in Figure 1(a). The antenna is etched on FR–4 substrate of dimensions L_{Sub} x W_{Sub} = 20 x 56 mm^2 and a thickness h = 1.6 mm. The relative permittivity of the substrate is $\varepsilon_r = 4.2$ and its loss tangent is tan $\delta = 0.01$. The substrate is partially backed by a ground plane with L_g = 10 mm, and $W_g = W_{Sub}$. The patch has a dimensions of L_p = 6 mm and W_p = 8 mm. The antenna is fed directly by a 50–microstrip line of width W_f = 3 mm, and length L_f = 7 mm printed on the top surface of the substrate. The feed gap (g) is used to adjust the impedance matching. The optimal chosen value of the gap width is 2 mm.

After optimizing the shape and size of the proposed UWB antenna, either one of two different planar EBG structures is added to the antenna to introduce a band rejection at 5–6 GHz band. The first is a slotted patch EBG (spEBG) structure added beneath the patch at the opposite side of the substrate. The spEBG structure consists of rectangular metallic patch with identical dimensions of those of the radiating patch but loaded with a resonant U–shaped slot. The slot has a uniform width of 1 mm, two vertical lengths $l_1 = l_2$ = 5 mm and a horizontal length l_3 = 7 mm. The slot is placed 0.5 mm away from the edge of the spEBG structure as shown in Figure 1(a). The second choice of an EBG structure is a parasitic strip EBG (psEBG) structure attached to the microstrip–line around the radiating patch as shown in Figure 1(b). The psEBG structure parameters are L_1 = 5.9 mm, L_2 = 4.45 mm, and $L_3 = L_4$ = 3 mm, and placed at L_5 = 2.8 mm from the top edge of the patch. The strip has a uniform thickness of 0.5 mm, and placed 0.5 mm away from the edges of the patch. The slot and strip dimensions are selected to optimize the required band–rejection performance. Photograph of the fabricated antennas are shown in Figure 2.

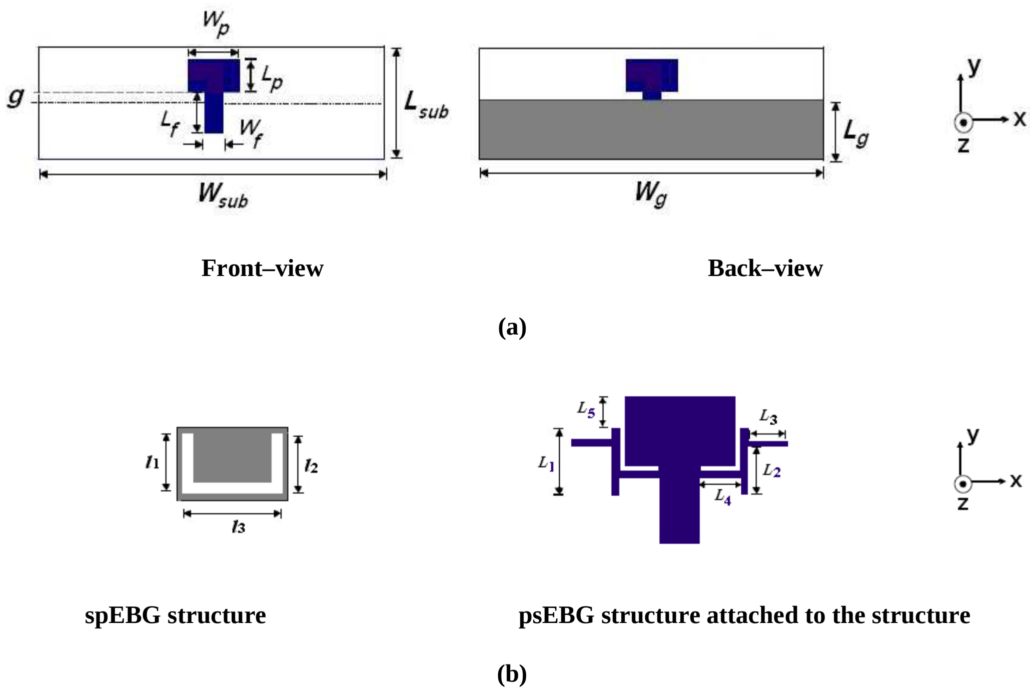

Figure 1. Geometry of the proposed band–notched UWB antenna. (a) Prototype antenna. (b) Proposed EBG structures.

ANTENNA PERFORMANCE

The proposed design is analyzed using Zeland IE3D which is based on the method of moments (MoM) numerical technique. Parametric analysis is adopted to optimize the proposed design. The antenna is fabricated using photolithographic technique and the measurements are performed with an Agilent HP8719 vector network analyzer. The simulated results and measured data of the reflection coefficient of the proposed antenna with the optimized dimensions without and with either one of the suggested EBG structures are shown in Figure 3. The measured data shows fairly good agreement with the simulated results. In spite of the resemblance of the simulated results and the measured data the minor deviation may be attributed to fabrication tolerance. During the parametric analysis it was observed that the proposed antenna is sensitive to the width of the ground plane, W_g. As the W_g increases, the lower limit of the frequency band increases, and hence the bandwidth of the antenna increases. The optimum value of W_g was found to be 56 mm, beyond which the effect is negligible. It is apparent that the prototype antenna can satisfy the UWB performance from 3.7 to beyond 10.6 GHz for VSWR$\leq$2 allocated by FCC for UWB communications. By incorporating either spEBG structure or psEBG structure in the design of the antenna a good band rejection characteristic at 5–6 GHz band is achieved. The EBG structures blocked the propagation of surface current at the band stop frequency due to its high impedance property. By adjusting and tuning the EBG structures, the desired band rejection performance can be achieved.

Front–view Back–view

(a)

Front–view Back–view

(b)

Figure: 2. Photograph of the fabricated antenna. (a) With spEBG structure. (b) With psEBG structure.

It is observed that by adjusting the length of the spEBG or psEBG structures of about one-half of the wavelength of the center frequency of the desired rejected band, destructive interference is maximized at that frequency which causes the antenna to be non-responsive. By increasing the total length of the slot or the strip of the EBG structures the notch frequency is shifted towards lower frequencies, and vice-versa.

The simulated radiation patterns of E_θ and E_φ in the yz and xz planes for the proposed antenna at frequencies 4 GHz and 7 GHz are illustrated in Figure 4. The patterns in the yz and xz planes are nearly omnidirectional. The radiating signal operating in the frequency band gap of the antenna with the EBG structures is suppressed reducing the antenna gain and radiation efficiency. Simulated results of the antenna peak gain versus frequency are shown in Figure 5. The gain varies from –3.18 dBi to 5.55 dBi over the operating frequency range of 3.1–10.6 GHz while it sharply reduced to reach -4dBi and -6dBi in the frequency rejection band (5–6 GHz).

SPICE–COMPATIBLE EQUIVALENT CIRCUIT

The rational approximation of a transfer function F(s) can be written as

$$F(s) = \sum_{k=1}^{N} \frac{res_k}{s - p_k} + d + se \tag{1}$$

Where $s = j\omega$ represents the complex frequency, res_k and p_k denote the k–th residue and pole, respectively, which may be either real quantities or complex conjugate pairs, and is extracted by using a fitting procedure such as, the Vector Fitting (VF) technique [18], d is constant term and e is the proportional term.

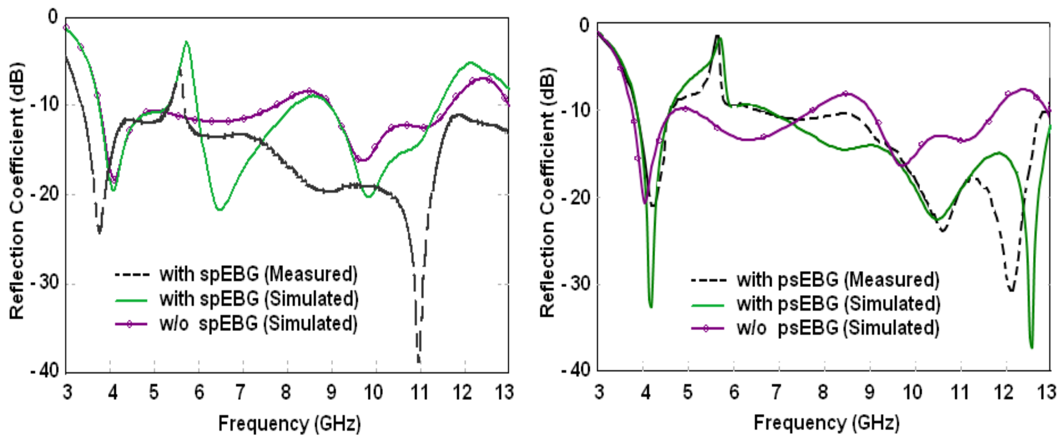

(a) **(b)**

Figure 3. Simulated and measured reflection coefficient versus frequency of the proposed antenna, (a) with spEBG structure. (b) with psEBG structure.

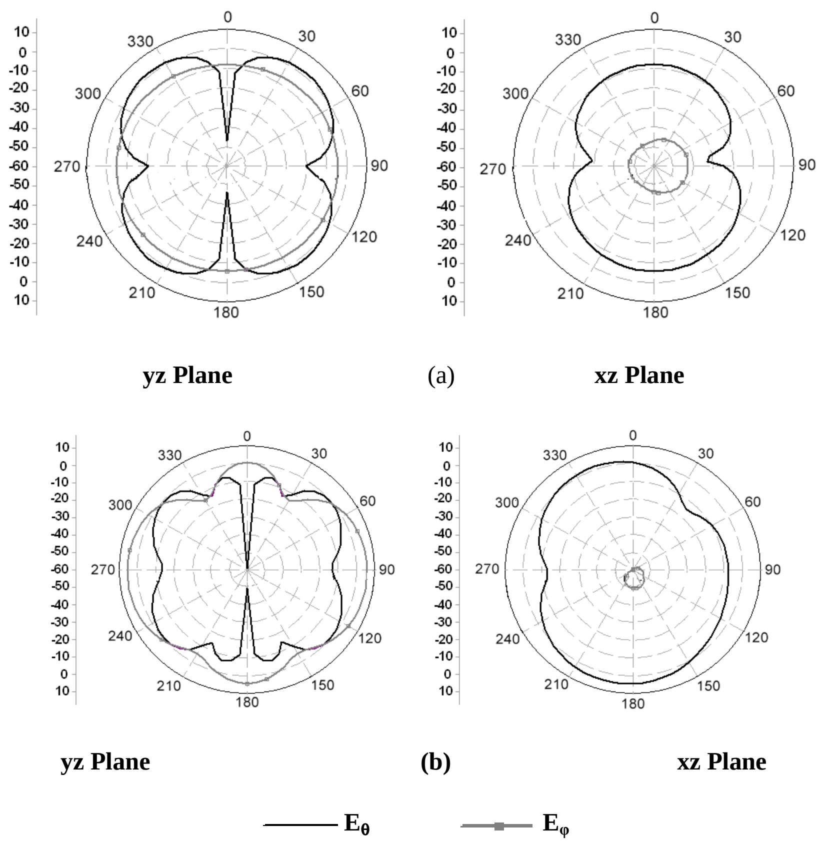

Figure: 4. Simulated radiation patterns of E_θ and E_φ in the yz and xz planes of the proposed antenna at, (a) 4 GHz. (b) 7GHz.

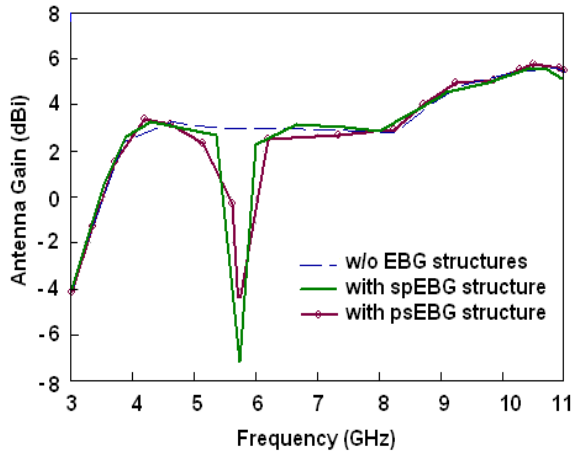

Figure: 5. Simulated peak gain versus frequency of the proposed antenna with and without the EBG structures.

We have the assumption that F(s) is an admittance–type function, the constant term d and the s–proportional one can be synthesized with a resistance and a capacitance whose values are 1/d and e. The equivalent circuit for the remaining part of F(s), res_k / s-p_k can be summarized as two cases [19].

Equivalent Circuit with Real Values of resk and p_k

Let's consider the RL series circuit in Figure 6. The admittance of the circuit can be easily calculated:

$$Y(s) = \frac{I(s)}{V(s)} = \frac{1}{R + sL} = \frac{\frac{1}{L}}{s + \frac{R}{L}} \tag{2}$$

The residue and pole of Y(s) are:

$$res_k = \frac{1}{L}, \ \ p_k = -\frac{R}{L} \tag{3}$$

So the R and L can be represented with res_k and p_k:

$$L = \frac{1}{res_k}, \ \ R = -\frac{p_k}{res_k} \tag{4}$$

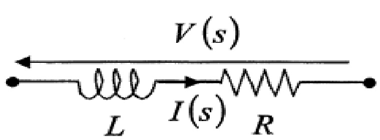

Figure: 6. Equivalent RL circuit for real poles synthesis

Equivalent Circuit with Complex Pair Values of res_k and p_k

Assume res_1, res_2, p_1 and p_2 are complex pairs, excluding the constant term and the s–proportional term, F(s) may be expressed as:

$$F(s)=\frac{res_1}{s-p_1}+\frac{res_2}{s-p_2}=\frac{(res_1+res_2)s-(res_1p_2+res_2p_1)}{s^2-(p_1+p_2)s+p_1p_2}=\frac{as}{s^2+sc+d}+\frac{b}{s^2+sc+d} \quad (5)$$

Where $$a=res_1+res_2;\quad b=-(res_1p_2+res_2p_1);\quad c=-(p_1+p_2);\quad d=p_1p_2 \quad (6)$$

Considering the RLC circuit, shown in Figure 7, which is a combination of a simple LR series circuit and a CR parallel circuit, the admittance of the circuit, in Figure 7, may be written in terms of its residues and poles as:

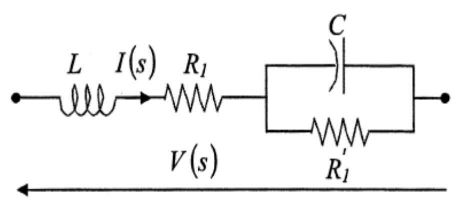

Figure: 7. Equivalent RLC circuit for complex pairs synthesis.

$$Y(s)=\frac{I(s)}{V(s)}=\frac{I(s)}{(sL+R_1)I(s)+\dfrac{R_1'\dfrac{1}{sC}}{R_1'+\dfrac{1}{sC}}I(s)}=\frac{1+sCR_1'}{s^2CLR_1'+s(CR_1R'+L)+R_1+R_1'}$$
$$=\frac{1}{L}\frac{(s+\dfrac{1}{R_1'C})}{(s^2+(\dfrac{R_1}{L}+\dfrac{1}{R_1'C})s+(\dfrac{R_1}{L}\dfrac{1}{R_1'C}+\dfrac{1}{LC}))} \quad (7)$$

Compared with Equation (5), the following relations can be achieved:

$$
\begin{aligned}
&res_1 + res_2 = \frac{1}{L} \\
&-(p_1 + p_2) = \frac{R_1}{L} + \frac{1}{R_1' C} \\
&p_1 p_2 = \frac{R_1}{L}\frac{1}{R_1' C} + \frac{1}{LC} \\
&-(res_1 p_2 + res_2 p_1) = \frac{1}{R_1' LC}
\end{aligned} \tag{8}
$$

The equations above can be solved and the RLC circuit parameters are:

$$
\begin{aligned}
&L = \frac{1}{res_1 + res_2} \\
&C = \frac{res_1 + res_2}{p_1 p_2 + \left[-(p_1 + p_2) + \dfrac{res_1 p_2 + res_2 p_1}{res_1 + res_2}\right] \times \left[\dfrac{res_1 p_2 + res_2 p_1}{res_1 + res_2}\right]} \\
&R_1 = \frac{1}{res_1 + res_2} \times \left[-(p_1 + p_2) + \frac{res_1 p_2 + res_2 p_1}{res_1 + res_2}\right] \\
&R_1' = -\frac{1}{C}\frac{res_1 + res_2}{res_1 p_2 + res_2 p_1}
\end{aligned} \tag{9}
$$

The complete equivalent circuit can be established as shown in Figure 8. C_0 represents the s–proportional one in F(s). R_0 is associated with the constant term in F(s). The RL series and the RLC combination circuit models can be selected according to the different two cases introduced above.

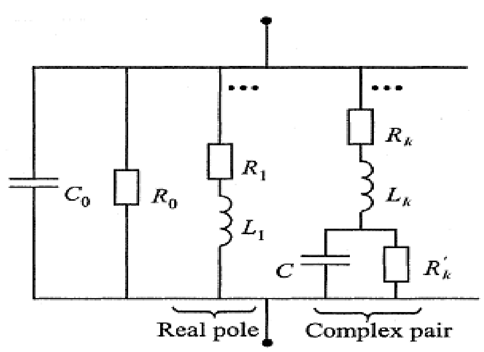

Figure: 8. SPICE-compatible equivalent circuit for antenna

Now this circuit modeling methodology is applied to obtain the equivalent circuit models of the input admittance of the proposed antenna without and with either one of the suggested EBG structures. First, the simulated input admittance of the proposed antenna was estimated. Second, the simulated input admittance was fitted by means of the Vector Fitting technique.

For the prototype antenna (without EBG structures), considering the tradeoff between the computational speed and accuracy, the initial number of poles in the VF procedure was chosen to be 18 linearly spaced complex poles and the number of iterations was 3. The fitting procedure has provided 9 complex pairs. The rational function approximation of Y(s) by VF is not shown here due to the limited number of pages. The proposed synthesis allows a satisfactory approximation of the input admittance, and the root-mean-square error (rms-error) on the magnitude is less than 4.9186e-006. The synthesized component values of the equivalent circuit for the prototype antenna are given in Table I. For the proposed antenna with spEBG structure by using 22 linearly spaced complex poles with 3 iterations, the fitting procedure has provided 11 complex pairs. The rms-error on the input admittance magnitude is less than 5.2315e-006. The synthesized component values of the equivalent circuit for the proposed antenna with spEBG structure are given in Table II. Finally, by using 22 linearly spaced complex poles with 3 iterations, the fitting procedure of the input admittance of the proposed antenna with psEBG has provided 11 complex pairs and the rms-error is less than 3.0591e-006. The synthesized component values of the equivalent circuit for the proposed antenna with psEBG structure are given in Table III.

In the equivalent circuit model, some resistors, conductors and capacitors are negative. According to [18], the resulting rational approximation may still have unphysical electrical components. Based on this circuit model, the effect of the antenna can be considered in the simulation of communication systems and it also helps designers to predict the system performance. The validity of the modeling method is verified and highly accurate results are obtained.

Table: 1. Synthesized Component Values for the Prototype Antenna

	The Equivalent Circuit Parameters					
No.	**L (H)**	**R (Ω)**	**C (F)**	**R\`(Ω)**	**R_0 (Ω)**	**C_0 (F)**
c1	4.33E-09	17.2408	5.78E-13	-669.7583		
c2	-4.17E-06	7.45E+04	-2.46E-16	-1.67E+05		
c3	5.81E-09	39.6562	1.92E-13	-4.99E+03		
c4	2.06E-08	2.02E+03	5.02E-15	-2.61E+03		
c5	4.80E-09	-83.4688	6.55E-14	635.4804	9.09E+01	-7.5422E-15
c6	8.21E-09	-47.205	3.00E-14	2.11E+03		
c7	8.40E-09	- 286.0393	1.73E-14	1.26E+03		
c8	1.17E-08	718.5737	8.38E-15	-2.32E+03		
c9	6.53E-10	132.514	3.51E-14	-231.2319		

Table: 2. Synthesized Component Values for the Proposed Antenna with $_{SP}$EBG Structure

No.	The Equivalent Circuit Parameters					
	L (H)	R (Ω)	C (F)	R`(Ω)	R_0 (Ω)	C_0 (F)
c1	4.13E-09	15.8037	6.21E-13	-651.5943		
c2	-1.19E-06	4.55E+03	-1.62E-15	-5.37E+04		
c3	6.11E-09	22.7195	1.90E-13	3.13E+03		
c4	3.10E-08	1.06E+03	1.30E-14	-2.31E+03		
c5	1.35E-08	854.2704	1.53E-14	-1.52E+03		
c6	5.59E-09	-142.7628	5.00E-14	610.5552	97.0874	3.01E-15
c7	8.89E-09	8.4177	2.82E-14	3.89E+03		
c8	9.79E-09	-452.1795	1.33E-14	1.35E+03		
c9	6.49E-07	2.70E+05	8.70E-18	-2.79E+05		
c10	7.31E-09	336.3397	1.52E-14	-1.80E+03		
c11	7.29E-10	129.9342	3.82E-14	-238.1938		

Table: 3. Synthesized Component Values for the Proposed Antenna with $_{PS}$EBG Structure

No.	The Equivalent Circuit Parameters					
	L (H)	R (Ω)	C (F)	R`(Ω)	R_0 (Ω)	C_0 (F)
c1	3.46E-09	8.6774	8.67E-13	-737.1287		
c2	7.39E-09	24.2417	1.68E-13	3.31E+03		
c3	7.39E-08	5.39E+03	3.08E-15	-7.52E+03		
c4	-1.65E-07	1.03E+04	-1.15E-15	-1.37E+04		
c5	3.34E-08	4.83E+03	1.50E-15	-5.38E+03		
c6	7.06E-09	-160.6566	4.13E-14	809.7998	106.383	1.42E-14
c7	-5.00E-05	8.39E+06	-6.24E-19	-9.32E+06		
c8	8.68E-09	112.9955	2.82E-14	-1.34E+04		
c9	5.12E-09	-42.0547	3.61E-14	1.55E+03		
c10	8.69E-09	1.2025	1.73E-14	1.19E+04		
c11	1.41E-09	258.2459	1.80E-14	-387.3913		

CONCLUSIONS

A novel design of a printed monopole antenna with a frequency band–notched characteristic for UWB applications is proposed and investigated. The band–notched is achieved by adding either a spEBG or a psEBG structure to the design of the antenna. The designed antenna satisfies VSWR requirement that is less than 2.0 in the frequency band from 3.7 to beyond 10.6 GHz, and shows band rejection characteristic at 5–6 GHz band. This rejected frequency band depends on the dimensions and the location of either one of the EBG structures. In this research the rejected frequency band is required to avoid interference with the existing WLAN communication system, which operates at this range of frequencies. The antenna is fabricated and the reflection coefficient versus frequency is measured. The measured data show good agreement with those obtained by simulations. With the help of vector fitting technique, SPICE–compatible equivalent circuit for the proposed antenna is established. The proposed antenna has a simple–shape and provides a good radiation pattern, relatively flat gain, and high efficiency over the entire frequency band excluding the rejected band.

REFERENCES

1. FCC Report and Order for Part 15 Acceptance of Ultra Wideband (UWB) Systems from 3.1–10.6 GHz, FCC, Washington, DC, 2002.
2. First Report and Order. Revision of part of the commissions rule regarding ultra wide band transmission system FCC02–48. Federal Communications Commission, 2002.
3. Eldek, A. A. Numerical analysis of a small ultra wideband microstrip–FED tap monopole antenna. Progress In Electromagnetics Research, Vol. 65, p. 59–69, 2006.
4. Yoon, H., H. Kim, K. Chang, Y. J. Yoon, and Y. H. Kim. A Study on the UWB antenna with band–rejection characteristic. IEEE AP–S Int. Symp., Monterey, CA, 2004, Vol. 2, p.1784–1787.
5. Choi, S. H., H. J. Lee, J. K. Kim. Design of an ultra–wideband antenna with band notch characteristic. IEEE AP–S Int. Symp., San Diego, USA, 2008, 1–4.
6. Liu, H.–W., C.–H. Ku, T.–S. Wang and C.–F. Yang. Compact monopole antenna with band–notched characteristic for UWB applications. IEEE Antenna and wireless propagation, Vol. 9, 397–400, 2010.
7. Sadeghzadeh, R. A., M. A. Honarvar, and A. R. Eskandari. Coplanar–fed UWB elliptical patch antenna with notched band characteristics. PIERS Proceeding, Xi'an, China, March 2010, 1225–1228.
8. Chung, K., J. Kim, and J. Choi. Wideband microstrip–fed monopole antenna having frequency band–notch function. IEEE Microwave and Wireless Components Letters, Vol. 15, No. 11, 766–768, 2005.

9. Gayathri, R., T. U. Jisney, D. D. Krishna, M. Gopikrishna, and, C. K. Aanandan. Band–notched inverted–cone monopole antenna for compact UWB systems. Electronics Letters, Vol. 44, No. 20, 1170–1171, 2008.

10. Khaled, E. E. M., A. A. R. Saad, and D. A. Salem. A proximity-fed annular slot antenna with different a band-notch manipulations for ultra-wide band applications. Progress In Electromagnetic Research B., Vol. 37, 289–306, 2012.

11. Khaled, E. E. M., A. A. R. Saad, and D. A. Salem. A proximity-fed ultra-wideband annular slot antenna with band-notch characteristics via a split-ring parasitic element. proc. 6th European Conference on Antennas and Propagation (EuCAP), Prague, March 2012, 1-5.

12. Yang, F. and Y. Rahmat–Samii, Electromagnetic Band Gap Structures in Antenna Engineering, New York: 2^{nd} Ed., Cambridge University Press, 2009.

13. Ayop, O., M. K. A. Rahim, M. R. Kamarudin, Aziz, M. Z. A. Abdul, and M. Abu. Dual band electromagnetic band gap structure incorporated with ultra–wideband antenna. Proc. of the Fourth European Conf. on Antennas and Propagation (EuCAP), Barcelona, Spain, 2010, 1–4

14. Dan, Q., and L. Shafai. The performance of microstrip patch antennas over high impedance EBG substrates within and outside its bandgap. Proc. IEEE Int. Symp. on Microwave Antenna Propagat. and EMC Technologies for Wireless Communications, MAPE 2005, 423–426.

15. Yang, F., and Y. Rahmat–Samii. Microstrip antennas integrated with electromagnetic band–gap (EBG) structures: A low mutual coupling design for array applications. IEEE Trans. Antennas Propagat., Vol. 51, 2939–2949, 2003.

16. Qi, L., H. M. Salgado, A. M. Moura, and J. R. Pereira. Dual–band antenna design using an EBG artificial magnetic conductor ground plane. Proc. IEEE Trans Antennas and Propagat. Conference, Loughborough, 2008, 217–220.

17. Coccioli, R., W. R. Deal, and T. Itoh. Radiation characteristics of a patch antenna on a thin PBG substrate. IEEE AP–S Int. Symp., 1998, Vol. 2, 656–659.

18. Gustavsen, B., and A. Semlyen. Rational approximation of frequency domain responses by vector fitting. IEEE Trans. Power Delivery, Vol. 14, No. 3, 1052–1061, July 1999.

19. Antonini, G. SPICE equivalent circuits of frequency-domain responses. IEEE Trans. Electromangnetic Compatibility, Vol. 45, No. 3, 502-512, August 2003.